Mechanism and Machine Theory 128 (2018) 528–543

Contents lists available at ScienceDirect

Mechanism and Machine Theory

journal homepage: www.elsevier.com/locate/mechmachtheory

Research paper

Power losses in power-split CVTs: A fast black-box approximate method

Dario Rotella, Marco Cammalleri*

Dipartimento dell'Innovazione Industriale e Digitale, Università di Palermo, Italia

ARTICLE INFO

Article history:
Received 22 March 2018
Revised 30 May 2018
Accepted 18 June 2018

Keywords:
Power split CVTs
Planetary gearing losses
Hybrid electric vehicles
GM voltec

ABSTRACT

This paper addresses the mechanical losses of planetary transmissions, with particular attention to power-split CVTs in their hybrid electric versions. It provides unified layout-independent analytical relationships, which can be used for both analysis, design and control purposes, and a simplified approach; the latter overcomes the necessity to segment the operating range of the power-split CVT in order to keep its loss model physically consistent. An example of application to a real hybrid electric PS-CVT is performed to show the simplicity, accuracy and generality of the proposed method.

1. Introduction

Step-less transmissions allow optimal operation of the prime engine, thus continuing to be one of the most promising solution for both the automotive and the motorcycling field [1–10]. Yet, the performance of the variator drive itself, whatever its type, can be improved considerably by means of the so-called power-split continuously variable transmission (PS-CVT), i.e. with the aid of a planetary gear system. PS-CVT has become almost a standard for earthmoving hydraulic machinery and drive the market of modern hybrid electric vehicles, for which the shafts of two reversible electric machines represent the variator drive [11–15].

More generally, in a PS-CVT (Fig. 1) we can discern between the continuously variable unit (CVU), i.e. a variator drive of any kind, and the power-split unit (PSU), i.e. a planetary gear system, possibly including both ordinary and planetary gear sets. By mean of the PSU, the size of the CVU can be reduced, the overall variable speed ratio range can be extended, and a better efficiency can be obtained in respect of using the same type of CVU, but working in series with the prime engine. The overall efficiency improvement can be significant when the efficiency of the CVU itself is low, since the gear sets in the PSU have a very high basic efficiency. Accordingly, the losses in the PSU are negligible for its preliminary design, if the latter is performed properly [16].

Nonetheless, assessing even small mechanical losses of the PSU can be important, because it allow the engineer to discriminate furtherly among the several functionally equivalent constructive solutions. In addition, it is essential for control purposes, as it permits to obtain the desired output power with the best overall efficiency. Determining power losses in planetary transmissions has attracted considerable interest in literature, mostly because power losses of a planetary gearing (PG), despite the high meshing efficiency between the involved gears, can be surprisingly high under specific circumstances. Indeed, it is well known that the meshing losses of a PG can be much worse than those of an ordinary gearing (OG) be-

* Corresponding author.
E-mail addresses: dario.rotella@unipa.it (D. Rotella), marco.cammalleri@unipa.it (M. Cammalleri).

https://doi.org/10.1016/j.mechmachtheory.2018.06.011
0094-114X/

Nomenclature

Acronyms

CVU	continuously variable unit
OG	ordinary gearing
PG	planetary gearing
PS-CVT	power-split continuously variable transmission
PSU	power-split unit
TPM	three-port mechanism

Subscripts

C, R, S	carrier, ring and sun of a PG
in, out, i, o	external shafts of the PSU
X, Y, Z	external shafts of a PG
x, y, z	external shafts of a TPM
j	jth shaft

Symbols

Over-lined	power or torque symbols refer to real working conditions of the PSU
P_j	ideal power transmitted by the jth shaft
p_j	dimensionless ideal power transmitted by the jth shaft
$P_j\|_n$	ideal power transmitted by the jth shaft of the nth TPM
$\bar{P}_{loss}$	power loss
$\bar{p}_L$	dimensionless power loss in the PSU
T_j	ideal torque applied to the jth shaft
η	overall apparent efficiency
η_v	CVU apparent efficiency
η_0	basic efficiency of a PG
$\eta^Z_{Y/X}$	fixed-Z apparent efficiency of a PG
$\eta^z_{y/x}$	fixed-z apparent efficiency of a TPM
$\eta_{X\|x}$	apparent efficiency of an OG linking the shaft x of the TPM to the shaft X of the PG
$\hat{\eta}$	unit vector of the overall apparent efficiency
Θ	dimensionless ideal output torque
θ_j	dimensionless ideal torque applied to the jth shaft
τ	overall speed ratio
τ_j	speed ratio of the jth shaft
$\tau_{\#j}$	overall speed ratio when the jth shaft is still
$\tau_{i\#o}$	τ_i when the shaft "o" is still
$\tau_{o\#i}$	τ_o when the shaft "i" is still
τ_*	overall speed ratio concurrent with the synchronism of a PG
$\hat{\tau}$	unit vector of the overall speed ratio
$\phi^z_{x/y}$	generalized characteristic function of a TPM
Ψ	reference Willis' ratio
ψ	constructive Willis' ratio
$\psi^Z_{Y/X}$	fixed-Z speed ratio of a PG
ω_j	angular speed of the jth shaft

cause the relative velocity between engaging teeth can be very high. Numerous methods claim to address any planetary transmission [17–23], nonetheless quantifying such losses remains a laborious task, especially when analyzing or designing compound PS-CVTs. Indeed, the use of convoluted and/or case-specific formularies can make their application very difficult. As a result, the study of PS-CVTs has been performed frequently neglecting the mechanical losses in the PSU [24–28] and in the CVU as well [29–32]. For instance, in [26] the problem of power recirculation, which is another way to explain the high losses of PGs, is addressed neglecting losses themselves. In [20] there is a remarkable attempt to provide a general approach to the problem of the PGs losses introducing the concept of reticulator and the responsivity theorem, yet, despite the formal analytical elegance of the solution, its application is not immediate. In [22] a systematic approach, based on the method proposed by [17] is described. Basically, it requires to identify the input and driven shafts, and then to calculate the overall efficiency of the PG depending on one experimental efficiency parameter and constructive ratio. Such parameter is then used to calculate the real power ratio between two shaft of the PG, and, definitively, to assess the power flow distribution. The same method is modified and elaborated furtherly in [23], splitting each simple planetary gear train in two basic ones and providing the relationships between powers as linear functions, but it remains conceptually the same. Unfortunately, it

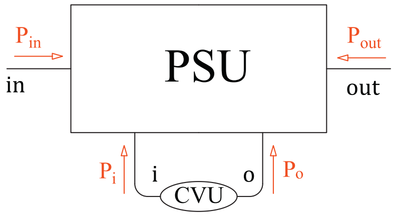

Fig. 1. General scheme of the PS-CVT.

introduces different cases depending on the internal power flows and constructive ratio of the PGs, which is not strictly necessary. Further remarks on the previous method can be found in [33,34]. In [35–38] the efficiency of simple shunt PS-CVTs in different configurations is analyzed, and several sources of discontinuities in the mechanical parameters are identified. In particular, [39] represents a specific work regarding the stall speed condition. [40] represents a recent theoretical and experimental study regarding the efficiency of a simple PG working in different conditions. In [41] a method analogous to [19] is proposed and applied to specific discrete planetary transmissions. In [42] several constructive solution are evaluated in terms of efficiency and reachable speed ratios. A brief, but very exhaustive review of some of the most influent meshing losses calculation methods is given [43]. Eventually, methods able to take into account also gears' elasticity [44] or churning, windage and bearing losses have been proposed in [45,46]. Experimental results about the spin losses have been given in [47].

Unfortunately, in most of the previous papers the research of a rigorous systematic approach has led to mathematical formalism, which makes the physical meaning of the intermediate results barely intelligible, and then the method themselves prone to errors. Others authors draw up encyclopedic formularies, which are hardly useful to the designer, particularly when the layout of the transmission is not definitive yet. Indeed, each shaft of a planetary gear set can be subject to torque and speed reversals, which may cause discontinuities in the mechanical loss factors of the linked devices. A rigorous study of the mechanical losses would require identifying and studying the conditions responsible for such discontinuities, making such task very tiresome, especially at earliest stage of the design process.

To overcome this problem, we suggest an approximated approach, which consents obtaining reliable results while ignoring such discontinuities, it being based on the physical coherence of the model. Indeed, we think that it is more fruitful for a designer being able to implement a general but simple method, which offers verisimilar results readily. In particular, our method is intended to address the mechanical losses of hybrid electric PS-CVTs, in which the shafts of the CVU represent a couple of reversible electric machines, but it can be easily applied also to hydraulic or mechanical CVUs, as well as to discrete planetary transmissions with any number of epicyclic gear trains.

2. Preliminary calculation of the power flows

In this section, we address the preliminary calculation of the power flows, both external (Section 2.1) and internal (Section 2.2) to the PSU. Indeed, as a general rule, this is necessary in order to keep the model physically consistent.

For this purpose, many authors count on the ideal power flow distribution, which is a reliable choice when the CVU apparent efficiency $\eta_v = -P_o/P_i$ is close to unity. However, when η_v is distant from unity the torque distribution is largely different, and several power flows change sign for transmission ratios very far from those predicted by the ideal model. Such condition can lead to inaccurate results, e.g. when the CVU is responsible for significant power losses, or if an energy accumulator is used to assist the prime engine or perform regenerative braking. Indeed, in these circumstances η_v can take values lower than zero or bigger than one, since its value is not strictly due to power losses. In general, throughout the paper, we define all the efficiencies as "apparent", because we keep unaltered their definition of power ratio between two shafts of the PS-CVT and no matter the underlying causes or the power flow directions. For these reasons, all the apparent efficiencies don't have to be comprised between 0 and 1.

However, in these circumstances, if we assume that only the losses in the planetary transmission are negligible at first, it is still possible to perform the preliminary calculation of the internal power flows and of the efficiency of the PS-CVT by mean of few general equations, using the method described in detail in [16,48]. Accordingly, we strongly recommend the use of the aforementioned method, since it does not imply any increase in computational complexity and it depends only on few functional parameters, as it will be clear in the next section.

2.1. Powers transmitted by the shafts external to the PSU

The mechanical points $\tau_{\#i}$ and $\tau_{\#o}$, i.e. the overall speed ratios when either the "i" or the "o" shaft of the CVU is blocked (see Fig. 1), permit calculating the relative power flows and torques on the main shafts of an ideal PSU directly by mean of the following relationships (1)–(3). Such relationships have been published in [48] as functions of the CVU apparent efficiency $\eta_v = -P_o/P_i$, while here they are expressed as functions of the overall apparent efficiency η instead, primarily

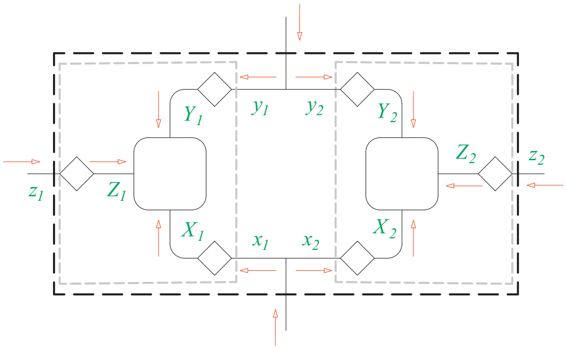

Fig. 2. Example of PSU with the four main shafts linked to two TPMs (left and right) and isokinetic joints (up and down). Squares and rhombi represent respectively planetary and ordinary gear sets. The capital letters refer to the shafts of the PGs, the lowercases to those of the TPMs. The arrows indicate the positive sign for the power flows, i.e. always entering their reference subsystem.

because this is the most appropriate logic when controlling electric PS-CVTs.

$$\tau = \frac{\omega_{out}}{\omega_{in}}; \quad \Theta = \frac{T_{out}}{T_{in}}; \quad \frac{P_{out}}{P_{in}} = -\eta \tag{1}$$

$$\tau_i = \frac{\omega_i}{\omega_{in}} = \tau_{i\#o} \cdot \frac{\tau - \tau_{\#i}}{\tau_{\#o} - \tau_{\#i}}; \quad \theta_i = \frac{T_i}{T_{in}} = -\frac{(1 + \Theta\,\tau_{\#o})}{\tau_{i\#o}}; \quad p_i = \frac{P_i}{P_{in}} = \frac{(\tau - \tau_{\#i})\,(1 + \Theta\,\tau_{\#o})}{\tau_{\#i} - \tau_{\#o}} \tag{2}$$

$$\tau_o = \frac{\omega_o}{\omega_{in}} = \tau_{o\#i} \cdot \frac{\tau - \tau_{\#o}}{\tau_{\#i} - \tau_{\#o}}; \quad \theta_o = \frac{T_o}{T_{in}} = -\frac{(1 + \Theta\,\tau_{\#i})}{\tau_{o\#i}}; \quad p_o = \frac{P_o}{P_{in}} = \frac{(\tau - \tau_{\#o})\,(1 + \Theta\,\tau_{\#i})}{\tau_{\#o} - \tau_{\#i}} \tag{3}$$

Each power is positive if entering the subsystem to which it refers, and the powers P_i and P_o can refer to either the CVU or the PSU (Fig. 1). Since the main object of this study is the PSU, hereinafter we assign them to the latter, but it is worth noting that, in order to change reference, it is enough to modify their sign in Eq. (2) and (3). For analogous reasons, we label as ideal the power flow distribution when we neglect the losses in the PSU, regardless what happens within the CVU. Eventually, we continue to refer to [48] for the kinematic relationships between the main shafts, i.e. τ_i, τ_o and τ.

2.2. Powers transmitted by the shafts internal to the PSU: generalized characteristic function

The mechanical points govern also a set of characteristic functions [16,48], which represent the ideal ratios between the powers transmitted by two shafts of a three-port mechanism (TPM), i.e. a simple planetary gear train with up to three fixed-ratio (see Fig. 2). In [16] we recommend their use for design purposes too, since they represent also the link between the synchronous conditions of the PGs and their respective Willis' ratios.

In [16] we have listed explicitly the basic characteristic functions for the design of PS-CVTs with up to two active planetary gear trains. However, in the current model it is neither necessary nor convenient to use a reference function, or to specify the internal layout of the PSU. Accordingly, we recommend to do not list them explicitly and we provide a general expression instead:

$$\phi^z_{x/y} = -\frac{P_y}{P_x} = \frac{\tau_y}{\tau_x} \cdot \frac{\tau_x}{\tau_y}\Big|_{\tau_z=0} = \frac{\tau - \tau_{\#y}}{\tau - \tau_{\#x}} \cdot \frac{\tau_{\#z} - \tau_{\#x}}{\tau_{\#z} - \tau_{\#y}} \tag{4}$$

In addition, a PSU involve two or more isokinetic joints, i.e. shafts belonging to different devices forced to spin with the same angular speed. For these joints is always valid the principle of conservation of power:

$$P_x\big|_1 + P_x\big|_2 + \ldots = 0 \tag{5}$$

As a result, two Eq. (4) for each TPM and one Eq. (5) for each isokinetic joint, together with Eq. (1)–(3), are sufficient in order to assess the ideal internal power flow distribution, for given input and output power, as described in the example of Section 7 and in [16,48].

As it can be easily verified, Eq. (4) can be deduced from the kinematic relations provided in Section 2.1, and it is possible to obtain whichever among the characteristic functions already listed in [16,48] by mean of simple substitutions, considering that $\tau_{\#out} = 0$ and $\tau_{\#in} = \infty$. Eventually, it is worth noting that this approach can be easily applied to the analysis of transmissions that involve more than two planetary gear trains (the number of possible characteristic functions raises factorially with the number of TPMs), such as complex multimode PS-CVTs or discrete automatic transmissions, provided that their mechanical points are known, or otherwise calculated as in [48].

3. Mechanical losses in the three-port mechanisms

As stated before, a TPM can be made of one planetary gear train and up to three ordinary gear sets (see Fig. 2).

In order to predict the mechanical losses of a TPM, we need to analyze the behavior of these devices separately and we refer to the shafts of the PG with the capital letters and to those of the TPM with the lowercase (see Fig. 2).

3.1. Losses in the planetary gear trains

In ideal conditions, for a planetary gear train the following equality is valid:

$$P_X + P_Y + P_Z = 0 \tag{6}$$

However, in real conditions, it is:

$$\bar{P}_X + \bar{P}_Y + \bar{P}_Z + \bar{P}_{loss} = 0 \tag{7}$$

If we continue to assume the powers as positive if entering their reference mechanism, it must be $\bar{P}_{loss} \leq 0$. If $\eta^Z_{Y/X}$ is the fixed-Z apparent efficiency, defined as follows:

$$\eta^Z_{Y/X} = -\frac{\bar{P}_Y}{\bar{P}_X}\Big|_{\omega_Z=0} = \frac{\bar{T}_Y}{\bar{T}_X} \cdot \frac{T_X}{T_Y} = \left(\frac{\bar{P}_Y}{\bar{P}_X}\right) / \left(\frac{P_Y}{P_X}\right) \tag{8}$$

accordingly, the real torque ratios are:

$$\frac{\bar{T}_Y}{\bar{T}_X} = -\frac{\eta^Z_{Y/X}}{\psi^Z_{Y/X}} \tag{9}$$

$$\frac{\bar{T}_Z}{\bar{T}_X} = \frac{\eta^Z_{Y/X} - \psi^Z_{Y/X}}{\psi^Z_{Y/X}} \tag{10}$$

in which $\psi^Z_{Y/X}$ is:

$$\psi^Z_{Y/X} = \frac{\omega_Y - \omega_Z}{\omega_X - \omega_Z} \tag{11}$$

Substituting the previous Eqs. (9)-(11) in (7), after some math, we obtain:

$$\bar{P}_{loss}\big|_{PG} = -\left(1 - \eta^Z_{Y/X}\right)(\omega_X - \omega_Z)\,\bar{T}_X \tag{12}$$

Since $\bar{P}_{loss} \leq 0$, according to Eq. (12), $\eta^Z_{Y/X}$ switches from lower to bigger than unity values, or vice versa, when:

- the planetary gear train reaches its synchronism.
- the torques transmitted by the shafts of the PG change sign.

Eventually, we can rewrite the latter in terms of characteristic functions, which are independent from the fixed gear joints (see Eq. (4) or [16,48]), and then equal for the PG and TPM, i.e. referable to the kinematic of the external shafts:

$$\bar{P}_{loss}\big|_{PG} = -\left(1 - \eta^Z_{Y/X}\right)\left(\frac{\phi^z_{x/y} - \psi^z_{x/y}}{1 - \psi^z_{x/y}}\right)\bar{P}_X \tag{13}$$

in which $\psi^z_{x/y} = \phi^z_{x/y}|_{\tau_*}$, and τ_* is the overall speed ratio for which the PG is synchronous [16].

Accordingly, we must assume that:

$$\begin{array}{lcl} \eta^Z_{Y/X} < 1 & & \left(\frac{\phi^z_{x/y} - \psi^z_{x/y}}{1-\psi^z_{x/y}}\right)\bar{P}_X > 0 \\ & if & \\ \eta^Z_{Y/X} > 1 & & \left(\frac{\phi^z_{x/y} - \psi^z_{x/y}}{1-\psi^z_{x/y}}\right)\bar{P}_X < 0 \end{array} \tag{14}$$

Usually, for a planetary gear train it is known the fixed-carrier efficiency, also known as basic efficiency, i.e. $\eta_0 = \eta^C_{R/S}$, where *R, C* and *S* represent the ring, carrier and sun gear of the PG. Considering that the torques applied to a PG are speed independent, the fixed-ring and fixed-sun efficiencies can be calculated by mean of the relationships of Table 1, in which $\psi = \psi^C_{R/S}$ is the Willis' ratio.

Assessing the real power ratios between the shafts of a PG requires calculating a pair of apparent efficiencies $\eta^Z_{Y/X}$ and $\eta^Y_{Z/X}$ (or $\eta^X_{Y/Z}$) by mean of Table 1, replacing *X,Y,Z,* with *R,C,S*, in the correct order, both for $\eta_0 < 1$ and for its reciprocal. The correct pair is selected accordingly to the previous test (14), which can be performed for only one of them, as they are mutually dependent and switch together. Eventually, when possible, it is better for $\bar{P}_X$ in Eq. (14) to be one of the two known main power flows of the PSU, such as $\bar{P}_{in}$ or $\bar{P}_{out}$, because they are supposed to do not change from the preliminary

Table 1
Relationships between fixed-shaft apparent efficiencies of a PG.

$\eta^C_{R/S}$	$\eta^C_{S/R}$	$\eta^R_{S/C}$	$\eta^R_{C/S}$	$\eta^S_{C/R}$	$\eta^S_{R/C}$
η_0	$\frac{1}{\eta_0}$	$\frac{1-\psi}{\eta_0-\psi}$	$\frac{\eta_0-\psi}{1-\psi}$	$\frac{\eta_0-\psi}{\eta_0\ (1-\psi)}$	$\frac{\eta_0\ (1-\psi)}{\eta_0-\psi}$

calculation. Indeed, for given input and output power, the PSU's mechanical losses will be compensated by the CVU, whose relative power flows will be different from those calculated by Eqs. (2) and (3). If the test cannot be performed with a known real power flow, the ideal one has to be used, but this could lead to mistakes within small ratio ranges in proximity of power flow inversions. Accordingly, in this case an iterative calculation may be necessary in order to obtain rigorous results.

3.2. Losses in the ordinary gears

For an ordinary gear (or wrapping pair), we can write:

$$\eta_{X/x} = \frac{\bar{P}_X}{\bar{P}_x} \tag{15}$$

Accordingly, losses in ordinary gear sets are simply:

$$\left.\bar{P}_{loss}\right|_{OG} = -\ \left(1 - \eta_{X/x}\right)\ \bar{P}_x \tag{16}$$

in which $\eta_{X/x}$ is the apparent efficiency of the ordinary gearing linking the shafts x, external to TPM, to the shaft X of the PG, and $\bar{P}_x$ is the power flowing in the xth shaft, positive if entering (see Fig. 2). Such losses have to be always negative as well, so when $\bar{P}_x$ changes sign, so does $(1 - \eta_{X/x})$:

$$\begin{matrix} \eta_{X/x} < 1 & & \bar{P}_x > 0 \\ & \text{if} & \\ \eta_{X/x} > 1 & & \bar{P}_x < 0 \end{matrix} \tag{17}$$

If the ordinary gearing itself is obtained using a PG with a fixed shaft Z, then it is possible calculating $\eta_{X/x} = \ \eta^Z_{X/x}$ by mean of the Table 1, replacing x, X, Z with R, C, S in the correct order.

4. Calculation of the real power flows

It is possible to follow the same procedure described in Section 2 in order to assess the real power flow distribution. As soon as the previous efficiency parameters have been calculated for each ordinary and planetary gear train, it is possible to correct the power ratios between the shafts of each TPM. Indeed, accordingly to Eqs. (4), (8) and (15), it is:

$$\frac{\bar{P}_y}{\bar{P}_x} = \eta^z_{y/x}\ \frac{P_y}{P_x} = -\left(\eta^Z_{Y/X} \cdot \frac{\eta_{X/x}}{\eta_{Y/y}}\right)\phi^z_{x/y} \tag{18}$$

Which is formally analogous to Eq. (4). Similarly, each isokinetic joint still provides the same power balance:

$$\left.\bar{P}_x\right|_1 + \left.\bar{P}_x\right|_2 + \ldots = 0 \tag{19}$$

Two Eq. (18) for each TPM and one Eq. (19) for each isokinetic joint, for given input and output power, are sufficient in order to assess the internal power flow distribution, including the real powers flowing through the shafts of the CVU.

5. Simplified approach

In this section, we describe an alternative simplified approach based on the results of Section 3, which eases the PSU's power loss calculation, makes superfluous performing the tests described in Section 3 itself, and permits calculating the real CVU's power flows directly and by mean of general scheme-independent expressions, as described in Section 5.3. Indeed, the method described in Sections 3 and 4 eventually leads to the exact result. Nevertheless, the process is often long and tiresome, especially in presence of multiple functioning modes, each one with its own synchronous conditions and power flow distribution.

In order to simulate passive devices (i.e. $\bar{P}_{loss} \leq 0$), $\eta^z_{y/x}$ is going to switch from lower to bigger than unity values, or vice versa, accordingly to the sign of speeds and applied torques (see Eqs. (14) and (17)). In other terms, the real power ratio (18) is going to be proportional to the ideal one, but in a discontinuous manner. Accordingly, it is necessary segmenting furtherly each functioning mode in order to model the behavior of the involved mechanical devices, which can show their torque discontinuities at different speed ratios. This leads to numerous variants of the analytical description of the model, making difficult a deep understanding of the problem and of the influence of its design variables. Furthermore, it may be necessary to perform the tests (14) and (17) by mean of the ideal power flow distribution at first, making an iterative approach necessary in order to obtain rigorous results.

For the above reasons, we propose in this section an approximate "blind" approach, derived from the previous one, but which allows the user to ignore such aspects at all, despite relying of the physical consistence of the model. In particular, a proper functioning of our simplified approach requires that the PSU mechanical loss, and then the deviation of $\eta^Z_{Y/X}$ from unity, is still minimal. Such occurrence is quite likely in practice for a PS-CVT [49], which is intended to enhance the performance of a CVU, especially if it is designed for hybrid electric applications. Nevertheless, it is well known that PGs with a constructive ratio ψ close to unity can show very low values of $\eta^Z_{Y/X}$, even if the basic efficiency η_0 of the PG is very high. For instance, considering acceptable only a value of $|1-\eta^Z_{Y/X}|<0.1$ (see next Eq. (20)), then, for an average basic efficiency of about $\eta_0\approx 0.95$, from Table 1 we get that all the existing transmissions with $0.5<\psi<1.5$ cannot be analyzed with the following simplified model. On the contrary, this approach can always be used at the design stage, because such Willis' ratios are already within a range to be absolutely avoided, as they provide the worst overall results (see Section 6).

5.1. Losses in the planetary gear trains

If $\eta_0\rightarrow 1$, when it switches to its reciprocal in Eq. (13), also the related value of $\eta^Z_{Y/X}$, calculated from Table 1, becomes about the reciprocal of the previous one. In addition, if we linearize the latter by mean of the Taylor formula, we obtain:

$$\frac{1}{\eta^Z_{Y/X}}\approx 2-\eta^Z_{Y/X} \tag{20}$$

Therefore, when η_0 switches, $\eta^Z_{Y/X}\rightarrow\frac{1}{\eta^Z_{Y/X}}\approx 2-\eta^Z_{Y/X}$, and the power loss Eq. (13) remains formally the same, except its sign. Moreover, since the mechanical losses are a small fraction of the power flows, their effects on the internal power flows are negligible. Therefore, it is safe to calculate the power losses only by mean of the ideal power flow distribution, i.e. assuming $\bar{P}_x\approx P_x$, as they will face even smaller absolute changes anyway. As a result, in Eq. (13), we can keep $\eta^Z_{Y/X}$ constant (its value can be either greater or lower than one) and write simply:

$$\bar{P}_{loss}\big|_{PG}\approx -\left|\left(1-\eta^Z_{Y/X}\right)\left(\frac{\phi^z_{x/y}-\psi^z_{x/y}}{1-\psi^z_{x/y}}\right)P_x\right| \tag{21}$$

since we know that power loss must be negative anyway. In conclusion, if the basic efficiency η_0 of PG is high as usual, and its Willis' ratio is far enough from unity, Eq. (21) permits to assess the PG's power loss in the whole operative range only by mean of the ideal power flow distribution and ignoring the switches of η_0, and thus those of $\eta^Z_{Y/X}$.

5.2. Losses in the ordinary gears

If a fixed-ratio joint is present in the three-port mechanism, and it can be subject to analogous simplification hypothesis of the PGs, its losses can be assessed by:

$$\bar{P}_{loss}\big|_{OG}\approx -\left|\left(1-\eta_{X/x}\right)P_x\right| \tag{22}$$

Such losses, summed to those of the planetary gear trains, qualifies the mechanical efficiency of the transmission.

5.3. Real CVU's power flows

Despite ignoring the changes in the internal power flow distribution in order to estimate the PSU's losses, it is still interesting to assess with sufficient precision the real power flowing through each shaft of the CVU. Indeed, as already stated above, for given input and output power, the PSU's mechanical losses will be compensated by the CVU, whose power flows will be slightly different from the ideal ones. If we normalize the mechanical power losses in respect of P_{IN}, we can write the following expressions:

$$\bar{p}_L=\sum\bar{p}_{loss}\big|_{PG}+\sum\bar{p}_{loss}\big|_{OG} \tag{23}$$

$$\bar{p}_i+\bar{p}_o=\bar{\theta}_i\ \tau_i+\bar{\theta}_o\tau_o=-(1-\eta+\ \bar{p}_L) \tag{24}$$

We can expect that the real torque ratios $\bar{\theta}_i$ and $\bar{\theta}_o$ applied to the shafts of the CVU, despite being different from their ideal values θ_i and θ_o, are still linear functions of $\Theta=-\eta/\tau$, just like θ_i and θ_o (see Eqs. (2) and (3)). Accordingly, in order to assess their new value, we can write a system of two equations, i.e. Eq. (24) and its directional derivative for which Θ is constant (and so $\bar{\theta}_i$ and $\bar{\theta}_o$ remain constant as well), which is in the direction of the vector $[{}^{\tau}_{\eta}]=\sqrt{\tau^2+\eta^2}[{}^{\hat{\tau}}_{\hat{\eta}}]$:

$$\begin{bmatrix}\tau_i & \tau_o\\ \frac{d\tau_i}{d\tau}\ \hat{\tau} & \frac{d\tau_o}{d\tau}\ \hat{\tau}\end{bmatrix}\begin{pmatrix}\bar{\theta}_i\\ \bar{\theta}_o\end{pmatrix}=\begin{pmatrix}\eta-1-\bar{p}_L\\ \hat{\eta}\ -\nabla\bar{p}_L\cdot\begin{bmatrix}\hat{\tau}\\ \hat{\eta}\end{bmatrix}\end{pmatrix} \tag{25}$$

Table 2
Apparent efficiency of the PG for different positions of the planet carrier.

Z	Y	X	$\psi(\Psi)$	$\eta^Z_{Y/X}(\psi)$	$\eta^Z_{Y/X}(\Psi)$	$\lvert 1-\eta^Z_{Y/X}\rvert$ for $\eta_0 \to 1$
C	R	S	Ψ	$\eta^C_{R/S} = \eta_o$	η_o	$\lvert 1-\eta_o\rvert$
S	C	R	$1-\frac{1}{\Psi}$	$\eta^S_{C/R} = \frac{\eta_o-\psi}{\eta_o(1-\psi)}$	$\frac{1-\Psi}{\eta_o}+\Psi$	$\lvert 1-\eta_o\rvert\ \lvert 1-\Psi\rvert$
R	S	C	$\frac{1}{1-\Psi}$	$\eta^R_{S/C} = \frac{1-\psi}{\eta_0-\psi}$	$(\frac{1-\Psi^{-1}}{\eta_o^{-1}}+\Psi^{-1})^{-1}$	$\lvert 1-\eta_o\rvert\ \lvert\frac{1-\Psi}{\Psi}\rvert$

After extensive math, we get:

$$\bar{p}_i = \bar{\theta}_i\ \tau_i = \ p_i - \bar{p}_L \frac{\tau_i}{\tau_{i\#o}} - \nabla\bar{p}_L \cdot \begin{bmatrix} \tau \\ \eta \end{bmatrix} \ p_i\Big|_{\eta=1} \tag{26}$$

$$\bar{p}_o = \ \bar{\theta}_o\tau_o = p_o - \bar{p}_L \frac{\tau_o}{\tau_{o\#i}} - \nabla\bar{p}_L \cdot \begin{bmatrix} \tau \\ \eta \end{bmatrix} \ p_o\Big|_{\eta=1} \tag{27}$$

in which $\nabla\bar{p}_L$ is the gradient of $\bar{p}_L$, defined as $\nabla\bar{p}_L = [\ \frac{d\bar{p}_L}{d\tau} \quad \frac{d\bar{p}_L}{d\eta}\ ]$, $p_o|_{\eta=1} = -p_i|_{\eta=1}$ and $\frac{\tau_i}{\tau_{i\#o}} = \frac{\tau-\ \tau_{\#i}}{\tau_{\#o}-\tau_{\#i}} = 1 - \frac{\tau_o}{\tau_{o\#i}}$ (see Eqs. (1)–(3)).

Once established the power transmitted by the CVU's shafts to the PSU (positive if entering in the latter), it would be possible to assess with precision also the real losses of the CVU, i.e. the electrical losses of the two electric machines, thus calculating the overall losses of the PS-CVT in its entirety. However, we do not perform it because it is not strictly necessary for the comprehension of our model, which is suitable for any type of CVU. In particular, calculating the electrical losses accurately would require simply to look up the efficiency map of each involved motor, inverter, battery pack etc. and check with which efficiency each device is able to deliver (or absorb) the required power at the required speed (known from the our model). In other terms, our method uncouples the electrical efficiency of the e-CVT from the power flow distribution (and related mechanical losses) of the planetary transmission, so that engineers can address the two problems separately.

Eventually, it is worth noting that, for given $\bar{p}_L$ and $\nabla\bar{p}_L$, Eqs. (26) and (27) are scheme independent, them relying only on functional parameters, and that they have been obtained with no simplifying assumptions (i.e. are formerly exact), so only the calculation of $\bar{p}_L$ is a possible source of errors. In theory, the reader may use any model to calculate $\bar{p}_L$, and then Eqs. (26) and (27) in order to obtain $\bar{p}_i$ and $\bar{p}_o$ directly. Moreover, if we calculate $\bar{p}_L$ as a function of Θ and τ (keeping its relationship with η implicit), then $\frac{d\bar{p}_L}{d\eta} = 0$, and the previous equations can be written as a simple, explicit and general relationship between power losses and power transmitted by the shafts of the CVU, regardless the complexity of the PSU itself:

$$\bar{p}_i = \ p_i - \bar{p}_L \frac{\tau_i}{\tau_{i\#o}} - \frac{d\bar{p}_L}{d\tau}\ p_i\Big|_{\eta=1} \tag{28}$$

$$\bar{p}_o = \ p_o - \bar{p}_L \frac{\tau_o}{\tau_{o\#i}} - \frac{d\bar{p}_L}{d\tau}\ p_o\Big|_{\eta=1} \tag{29}$$

6. Difference of efficiency between functionally equivalent solutions

In [16] we have performed the design of PS-CVT based on normalized functional parameters neglecting the mechanical losses in the PSU. It has been shown that these functional parameters govern the kinematics and the ideal power flow distribution, and they can lead to numerous constructively different solutions. In particular, functionally equivalent TPMs could be obtained with three different Willis' ratios, according to the position of the planet carrier. In this section, we are going to show which of the three possible choices can achieve better results, i.e. lower mechanical losses, keeping unaltered the functional parameters.

In particular, in the previous sections, we have shown that the mechanical losses of a PG, for given functional parameters (i.e. kinematics and ideal power flows), depend mostly on the parameter $\eta^Z_{Y/X}$, which is just function of the position of the planet carrier (and the related constructive Willis' ratio see Eq. (13) and Table 1). Accordingly, in order to compare the efficiency of the three possible constructive solutions, we have to:

- take one of them (and its constructive Willis' ratio Ψ) as a reference.
- calculate in function of Ψ the constructive Willis' ratios ψ of the other two solutions according to the position of their planet carriers.
- calculate their respective parameters $\eta^Z_{Y/X}$ from Table 1.
- express the same parameters $\eta^Z_{Y/X}$ as functions of Ψ to ease the comparison.
- approximate the results to get general design guidelines.

Namely (see Table 2), if we choose X, Y, Z as reference positions for sun S, ring R (or second sun), planet carrier C, and consequently $\Psi = \psi^Z_{Y/X}$ as reference for the Willis' ratio, then Eq. (11) leads to the column $\psi(\Psi)$ while the relationships of

Table 1 lead to the column $\eta^Z_{Y/X}(\psi)$. Then, replacing the content of the column $\psi(\Psi)$ in the column $\eta^Z_{Y/X}(\psi)$, we get the column $\eta^Z_{Y/X}(\Psi)$. The latter would make possible comparing exactly the loss factor of a given transmission (taken it as a reference, first row) with the other two possible constructive solutions (second and third row).

Indeed, the farther would be the value of $\eta^Z_{Y/X}(\Psi)$ from unity, calculated both for $\eta_o < 1$ and for its reciprocal, the worst would be the losses related to that constructive solution. It is worth noting that, to be faultfinding, η_o could change from one constructive solution to another because of the different number of meshing pairs necessary to realize certain values of the constructive Willis' ratio $\psi(\Psi)$ (and a proper ring gear may not be present as well).

However, considering that the basic efficiency η_0 is generally high (see Section 5.1), it is possible to simplify the results to get some general design guidelines. In particular, if $\eta_o \to 1$, following the same procedure exemplified by Eq. (20), we get the last column of Table 2. The latter, together with the column $\psi(\Psi)$, shows clearly that whichever is the value of the reference Willis' ratio Ψ, two out of the three possible solutions have their constructive Willis' ratio $\psi(\Psi) > 0$ and both are worse than that with $\psi(\Psi) < 0$.

In addition, from a more in-depth analysis of the same functions, it results that the worst of the two solutions with $\psi > 0$ is the one requiring $0.5 < \psi < 2$, which is obtained if the carrier of the PG is linked to the shaft that should be connected to the sun of the PG with $\psi < 0$ (see Section 7.3 for an example).

For the above reasons, we suggest to try to limit the design chart to the negative values of the Willis' ratio, as we did in [16]. If a negative Willis' ratio is not feasible, the designer can try, at worst, to connect the carrier to the ring position of the ideally optimal (but not feasible) solution. In other terms, it is strongly recommended to exclude the possibility of using constructive Willis' ratios in the range $0.5 < \psi < 2$ as early as in the preliminary design process.

7. Example

In this section, we return to the example already examined in detail (but neglecting mechanical losses) in [48], and we apply our simplified method to the Voltec PS-CVT (Fig. 3).

The Voltec offers two PS-CVT modes, and the switch between them occurs when motor A (the shaft "i") is still. It can perform also a fixed-ratio parallel mode or a FEV mode, which can be considered sub-cases of the PS-CVT functioning [48]. The mechanical points, calculated in [48] are listed in Table 3 (see also Fig. 4):

The final drive is made of a wrapping pair (a chain drive) linked to the sun of a fixed-ring PG, whose carrier is linked to the final differential, for an overall final drive ratio $k_{out} = \frac{1}{2.64} = 0.379$.

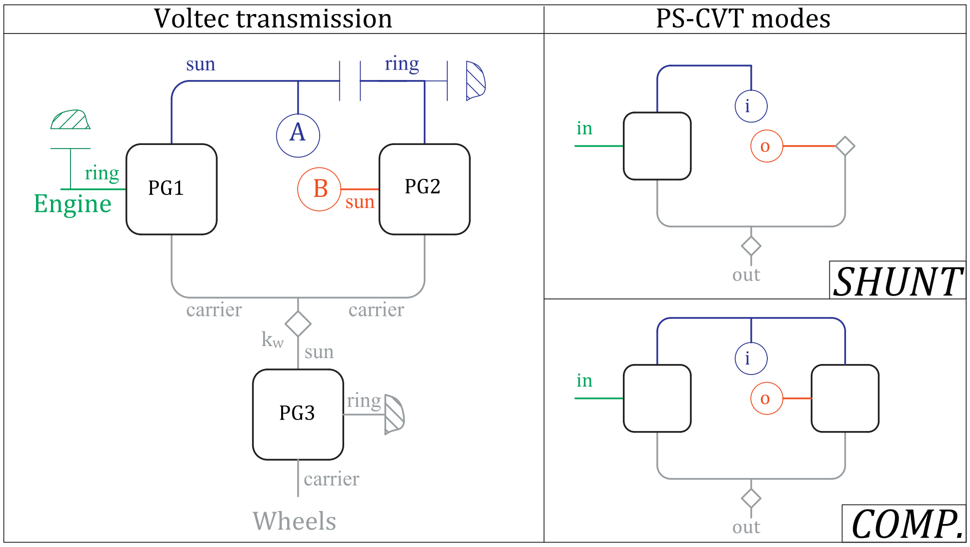

Fig. 3. GM Voltec: constructive and functional schematics.

Table 3
Functional parameters of the Voltec transmission.

Mode	$\tau_{\#i}$	$\tau_{o\#i}$	$\tau_{\#o}$	$\tau_{i\#o}$
Shunt	0.247	2.00	0	−1.87
Compound	0.247	2.00	0.510	2.00

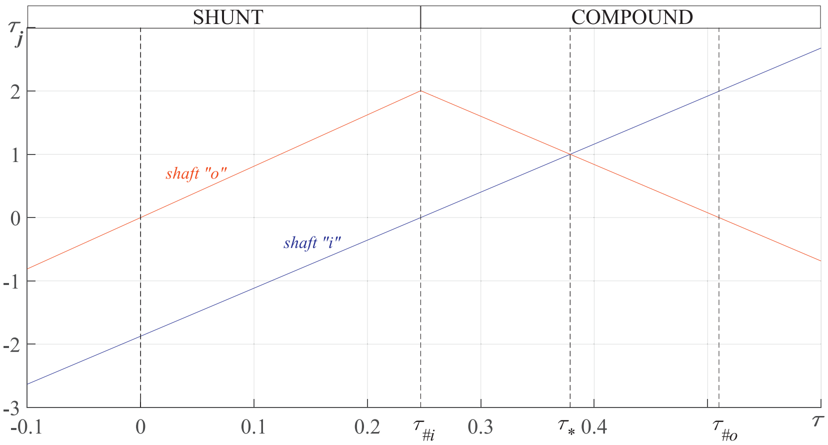

Fig. 4. Kinematic relationships between the main shafts of the Voltec.

Since no other ordinary gears are involved, in the compound mode the synchronous condition is common to the planetary gear trains PG1 and PG2 and occurs for $\tau_* = k_{out} = 0.379$, which is between the mechanical points. Conversely, in the shunt mode, PG1 maintains the same synchronous ratio, but PG2 has become a fixed ratio gearing.

7.1. Application of the simplified model

The power losses are:

$$\bar{p}_L = \left.\bar{p}_{loss}\right|_{PG1} + \left.\bar{p}_{loss}\right|_{PG2} + \left.\bar{p}_{loss}\right|_{OG}$$

where, by Eqs. (21)–(22),

$$\left.\bar{p}_{loss}\right|_{PG1} = -\left|\left(1-\eta_{I/IN}^{OUT}\right)\left(\frac{\phi_{in/i}^{out}-\psi_{in/i}^{out}}{1-\psi_{in/i}^{out}}\right)\ p_{in}\right|$$

$$\left.\bar{p}_{loss}\right|_{PG2} = -\left|\left(1-\eta_{I/O}^{OUT}\right)\left(\frac{\phi_{o/i}^{out}-\psi_{o/i}^{out}}{1-\psi_{o/i}^{out}}\right)\ p_{o}\right|$$

$$\left.\bar{p}_{loss}\right|_{OG} = -\left|\left(1-\eta_{OUT/out}\right)\ p_{out}\right|$$

Accordingly, in order to assess the power losses, we do not need to perform a thorough preliminary power-flow calculation, but we can rely entirely on Eq. (3) for the calculation of p_o, since $\bar{p}_{in} = p_{in} = 1$ by definition and $\bar{p}_{out} = p_{out} = -\eta$ is our input known parameter. As regards the other parameters, the characteristic functions and the related constructive parameters are calculated by mean of Eq. (4). In particular, for the compound mode, it is:

$$\phi_{in/i}^{out} = \frac{\tau-\tau_{\#i}}{\tau-\tau_{\#in}}\cdot\frac{\tau_{\#out}-\tau_{\#in}}{\tau_{\#out}-\tau_{\#i}} = \lim_{\tau_{\#in}\to\infty}\frac{\tau-0.247}{\tau-\tau_{\#in}}\cdot\frac{0-\tau_{\#in}}{0-0.247} = 1-\frac{\tau}{0.247}$$

$$\psi_{in/i}^{out} = \phi_{in/i}^{out}(\tau_*) = \phi_{in/i}^{out}(0.379) = -0.536 = \psi_1$$

$$\phi_{o/i}^{out} = \frac{\tau-\tau_{\#i}}{\tau-\tau_{\#o}}\cdot\frac{\tau_{\#out}-\tau_{\#o}}{\tau_{\#out}-\tau_{\#i}} = \frac{\tau-0.247}{\tau-0.510}\cdot\frac{0-0.510}{0-0.247} = \frac{\tau-0.247}{\tau-0.510}\cdot 2.065$$

$$\psi_{o/i}^{out} = \phi_{o/i}^{out}(\tau_*) = \phi_{o/i}^{out}(0.379) = -2.077 = \frac{1}{\psi_2}$$

As regards the apparent efficiencies, we assume a mean meshing pair efficiency of about 0.98, and then a basic efficiency $\eta_0 = 0.96$ for all the PGs. We don't need to use Table 1 for PG1 and PG2, since the output shaft is linked to both their carriers, and then we can write simply $\eta_{I/IN}^{OUT} = \eta_{I/O}^{OUT} = 0.96$.

The calculation of $\eta_{OUT/out}$ is more articulated as it is the results of two devices. The final drive ratio is $k_{out} = 0.379$, therefore, assuming that the wrapping pair ratio is $k_w = 1.2$, the constructive ratio of PG3 results $\psi_3 = -0.461$. From Table 1 we can obtain its apparent efficiency, which is equal to

$$\eta_{S/C}^{R} = \frac{1-\psi_3}{1/\eta_o-\psi_3} = 0.972$$

Accordingly, if the wrapping pair ratio efficiency is $\eta_w = 0.98$, it is $\eta_{OUT/out} = 0.953$.

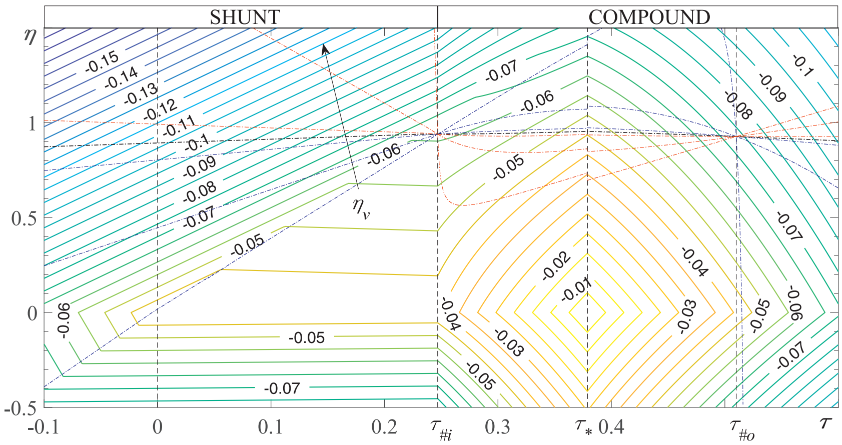

Fig. 5. Mechanical losses (as a fraction of the input power).

The only parameter that we need to modify in order to address the shunt mode is the value of $\tau_{\#o}$ (see Table 3), which modifies just p_o and $\phi_{o/i}^{out}$ accordingly to Eqs. (3) and (4). The Willis' ratios are constructive teeth ratios and do not change.

In Fig. 5 we have plotted the contour map of the mechanical loss as a fraction of the input power for different values of the overall apparent efficiency η and the overall speed ratio τ, i.e. of the dimensionless output power and speed. As it could be expected, the power losses show an absolute minimum in correspondence of the synchronous condition and for null values of the output power (i.e. $\tau = \tau_* = 0.379$ and $\eta = 0$). On the contrary, the mechanical losses can be significant for $\eta > 1$ (e.g. during assisted acceleration) and $\eta < 0$ (e.g. during regenerative braking), since such conditions imply more power circulating within the PSU, and they are generally worse for the shunt mode because of the bigger working distance of the PG1 from its synchronous condition.

The dash-dot lines represent points of functioning for which the ratio $\eta_v = -p_o/p_i$ between the powers flowing through the shafts of the CVU is constant (blue for $0 < \eta_v < 1$ and red for $1 < \eta_v < \infty$). In order to keep the figure clear, we have represented only the curves related to $\eta_v = 0.02,\ \eta_v = 0.5,\ \eta_v = 0.9,\ \eta_v = 1$ and their reciprocals. In correspondence of the mechanical points, all these curves intercept in a point, which is representative of the fixed-ratio efficiency of the transmission; indeed, in this condition, finite values of η_v imply that an electric motor is kept still and the other runs unloaded. Vice versa, if the latter is supplying power, η_v is not finite and for this speed ratio the value of $\bar{p}_L$ can change accordingly to η (parallel mode).

In correspondence of the stall speed ($\tau = 0$) the overall apparent efficiency η must be null, since is null the speed of the output shaft. Such condition is indeed intercepted by the dash-dot curve for $\eta_v \to 0$, because, for $\tau = 0$ in the shunt mode, the shaft "*o*" must be still as well. Yet, the values of $\bar{p}_L$ for $\tau = 0$ and $\eta \neq 0$ represent the limit conditions for low values of both input and output powers; indeed, for values of $\tau \to 0$, η_v and η can be different from zero. In conditions of battery charge sustaining ideally it would be $\eta_v = 1$, but because of the electrical losses we can expect $\eta_v \approx 0.9$, or its reciprocal, and then a roughly constant output power is obtained in most of the operative range (such condition is represented by the closest dash-dot line below the black one).

The data necessary to build the map of Fig. 5 are also sufficient in order to assess the real power flows flowing through the electric path, by mean of Eqs. (26) and (27). In particular, the normalized power flowing through the shaft "*i*" is Fig. 6 and the one through the shaft "*o*" is Fig. 7.

Despite the gradient of the mechanical loss $\bar{p}_L$ shows numerous discontinuities, the value of the function itself remains continuous and it causes a small jump for both $\bar{p}_i$ and $\bar{p}_o$ only in correspondence of the synchronous condition. Nonetheless, it should be possible to cross the synchronous condition without abrupt changes of the CVU torques or of the output torque by gradually modifying $\bar{p}_i$ and $\bar{p}_o$, while maintaining their sum constant accordingly to Eq. (24).

Yet, it is worth noting that, since the maps of Figs. 5–7 are normalized in respect of the input power and speed, the actual boundaries of the operating points may be narrower of those shown in the figures. Indeed, for each target absolute output speed and power, each couple of variables τ, η define a specific absolute input speed and power (i.e. operating conditions of the i.c. engine), and then also the required absolute speed and power of the electric motors by mean of the relationships plotted in Figs. 6–7. As a result, it is possible to restrain the range of feasible operative conditions accordingly to the operative limits of the three power units, and to select the optimal working condition combining their own efficiency maps with that of $\bar{p}_L$. Similarly, it would be possible to use the previous results in order to redesign a transmission, i.e. refine the values of $\tau_{\#i}$ and $\tau_{\#o}$ obtained by mean of the preliminary calculations suggested in [16] in order to fit the real power flow distribution and/or a more specific control strategy. In addition, the normalization of results in respect of the input power implies that they are equally valid when P_{IN} is negative, i.e. when the electric motors are both driving the car and cranking the i.c. engine.

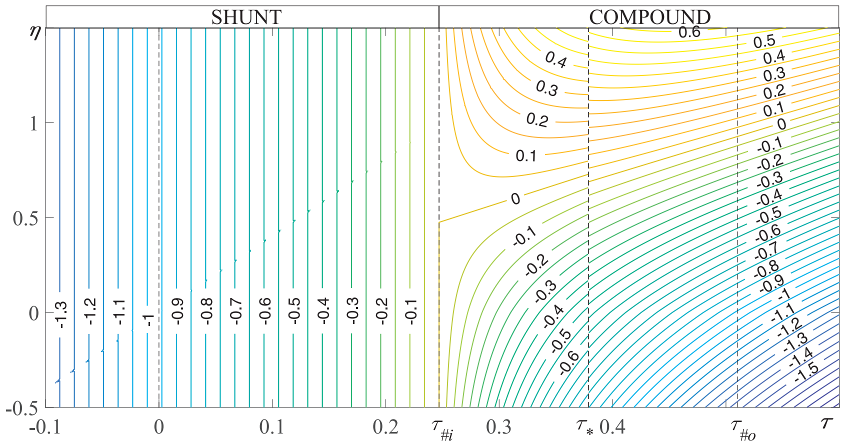

Fig. 6. Power transmitted by the shaft "*i*" (as a fraction of the input power).

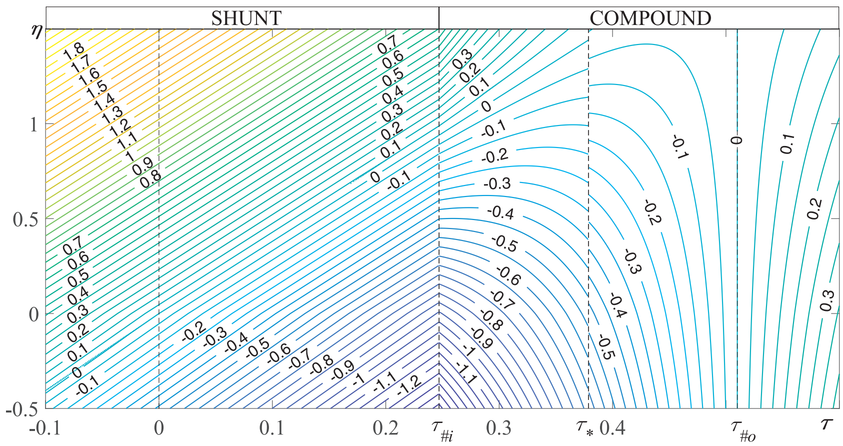

Fig. 7. Power transmitted by the shaft "*o*" (as a fraction of the input power).

Eventually, Fig. 8 highlights where the gradient of mechanical loss $\bar{p}_L$ (Fig. 5) shows discontinuities. In particular, it shows the boundaries between zones in which the apparent efficiency of the involved mechanical devices should have switched due to some reversal of torque, speed or power on their shafts.

Despite the Voltec transmission is reasonably simple (just two operative modes, up two power-split PGs and no ordinary gears internal to the PSU), there are nine zones within the studied interval, but far more are possible for slightly more complex PS-CVTs. Thanks to our simple model, there is no need to predetermine such zones or perform any switch.

7.2. Model accuracy compared to numerical simulation

We have simulated the transmission in Simulink Simscape for different values of overall apparent efficiency η (for $\eta =$ 1.5, 1, 0.5, 0, -0.5) in order to verify the accuracy of the proposed model. Indeed, a comparison only between exact and approximate analytical results would only prove that we have performed the approximation properly, but not that our model itself is correct. Vice versa, comparing our results (both exact and approximated) directly with a simulation supports that our predictions are correct.

The Simulink model is built using the physical blocks of the Simscape driveline toolbox, without using any additional customized analytical model. The input parameters of the simulation (teeth ratios, efficiency of gear pairs etc.) are obviously the same of the model.

Figs. 9–13 show the comparison between simulated points (markers) and calculated points (solid lines for the approximated method, dotted lines for the exact one), for both the overall mechanical loss (left) and for the power flowing through the electric motors (right). As usual, the blue lines refers to the main shaft "*i*" (motor A) and the red ones refers to the main shaft "*o*" (motor B).

As it can be observed, for Figs. 9–13 the error in the assessment of the power loss is within the fraction of centesimal, while the error for both $\bar{p}_i$ and $\bar{p}_o$ is not noticeable. The exact and the simulated result coincide, but the simulation offers

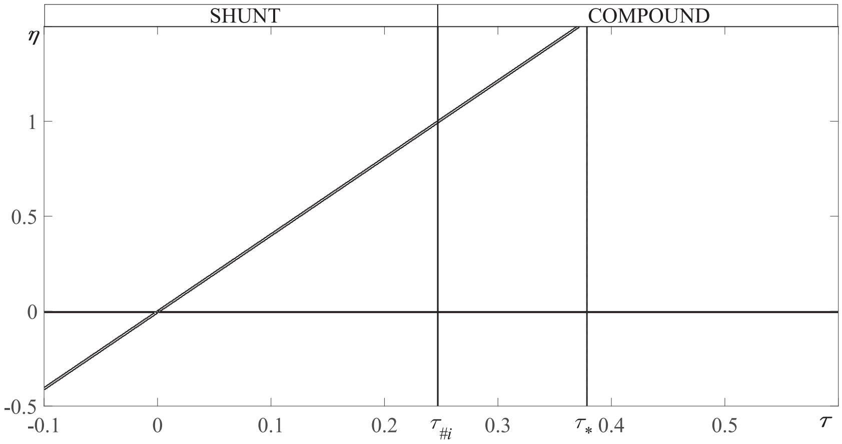

Fig. 8. Transition zones of the constructive efficiency parameters.

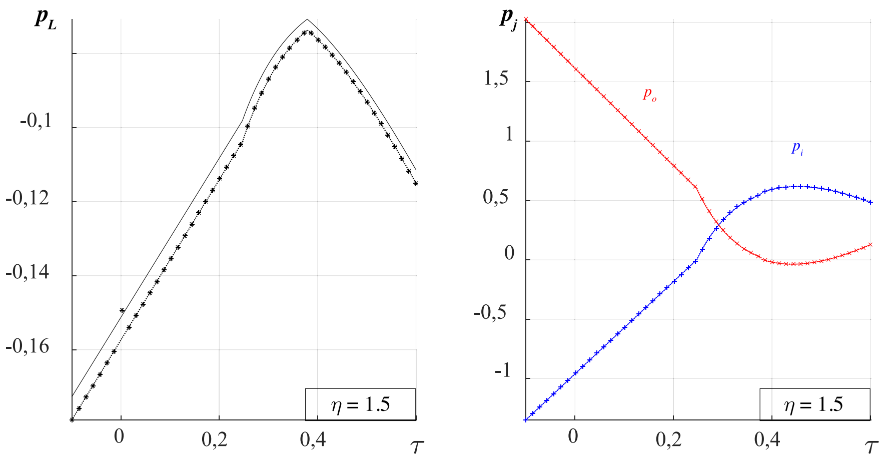

Fig. 9. Simulated (markers) and calculated (solid lines) mechanical losses (left) and CVU's power flows for $\eta = 1.5$.

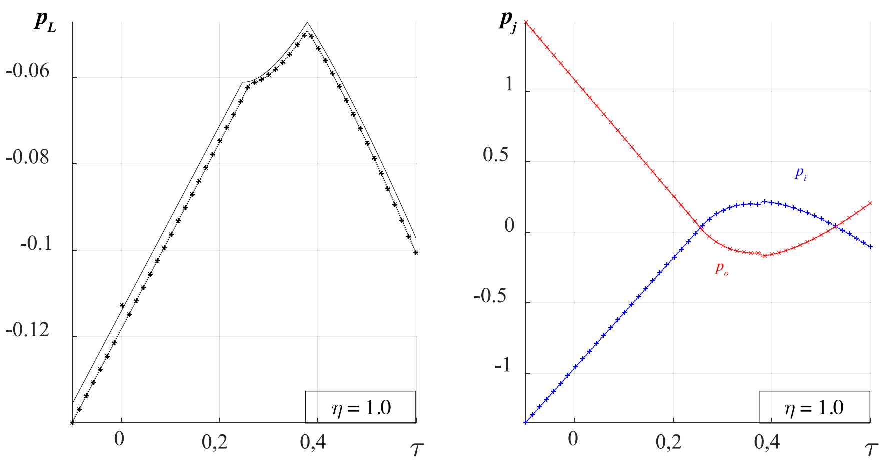

Fig. 10. Simulated (markers) and calculated (solid lines) mechanical losses (left) and CVU's power flows for $\eta = 1.0$.

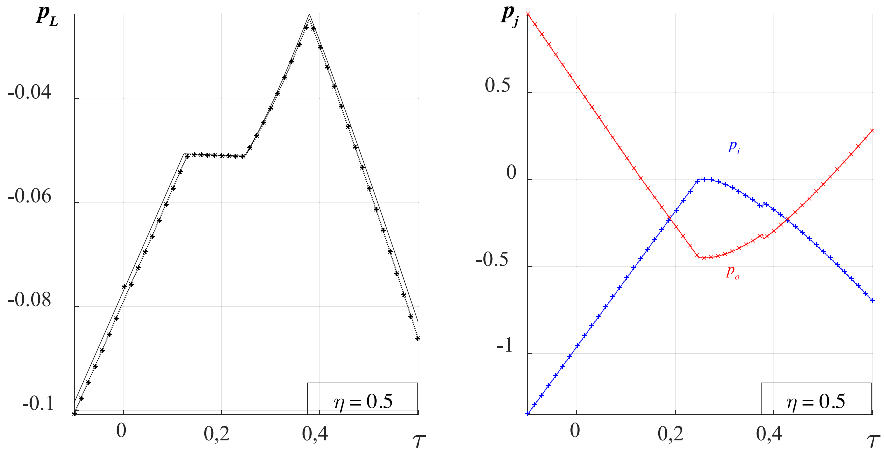

Fig. 11. Simulated (markers) and calculated (solid lines) mechanical losses (left) and CVU's power flows for $\eta = 0.5$.

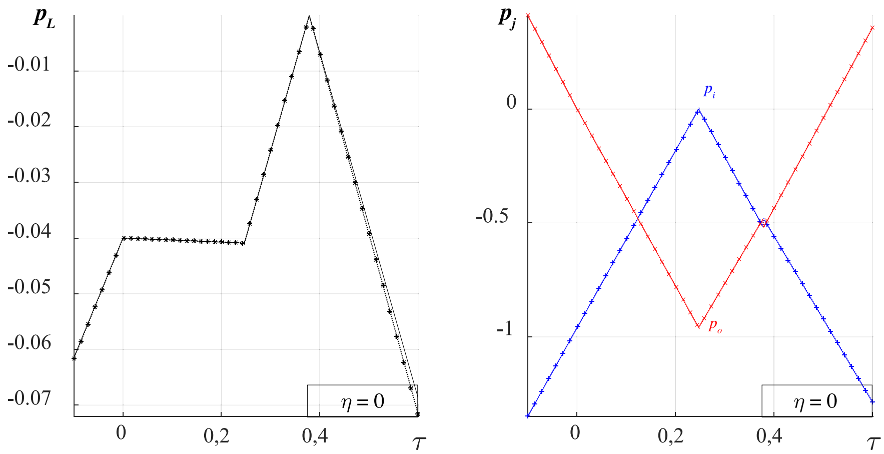

Fig. 12. Simulated (markers) and calculated (solid lines) mechanical losses (left) and CVU's power flows for $\eta = 0$.

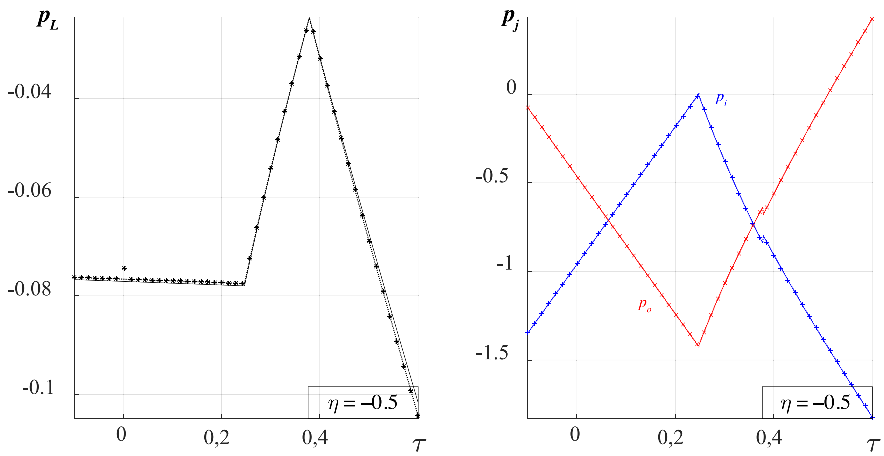

Fig. 13. Simulated (markers) and calculated (solid lines) mechanical losses (left) and CVU's power flows for $\eta = -0.5$.

Table 4
Comparison between constructively different solutions for PG1.

$Z \equiv out$	$Y \equiv in$	$X \equiv i$	$\psi(\Psi)$	$\lvert 1-\eta^{Z}_{Y/X}\rvert$ for $\eta_0 \to 1$
C	R	S	−0.536	$\lvert 0.04\rvert$
S	C	R	2.87	$\lvert 0.04\rvert\,\lvert 1.54\rvert$
R	S	C	0.651	$\lvert 0.04\rvert\ \lvert -2.87\rvert$

irregular results near the stall speed except for $\eta = 0$, and this is due to the aforementioned reasons, i.e. because $\eta \neq 0$ for $\tau = 0$ implies applying infinite absolute torques to the model if the prime engine is not idling, while the blocks in Simulink Simscape are supposed to work with finite dimensional physical inputs; definitively, our analytical model seems to be more resilient in such limit conditions.

7.3. Evaluation of other constructive solutions

With reference to Section 6, in this section we assess the effects of a change of the position of the planet carrier in a PG of the Voltec (and thus choosing a kinematically equivalent, but constructively different gear set).

For instance, if we try to calculate Table 2 for PG1, we obtain the results of Table 4 which are in plain accordance with what we have stated in Section 6: the current solution is optimal because the Willis' ratio is negative, and the worst scenario would be the third one, implying $0.5 < \psi < 2$, which is when the planet carrier is linked to the shaft "*i*", to which it is linked the sun gear of the current optimal solution with $\psi < 0$.

In particular, the choice of $\psi = 0.651$ would cause a $+187\%$ in the losses of PG1 in the whole operative range. Similar results can be obtained for PG2, since its Willis' ratio is -0.481.

8. Results and discussion

In [16], we provide a general method for the design of PS-CVTs by mean of few functional parameters, but neglecting the mechanical losses in the planetary transmission (PSU). In [48] we suggest a method for the calculation of these functional parameters for known PS-CVTs.

In this paper, we describe a method for the assessment of the mechanical losses in the PSU, which relies on the aforementioned functional parameters (mechanical points). In particular, in Section 7, we apply our simplified approach to the Voltec transmission, which we had already analyzed in [48] neglecting mechanical losses. As it can be observed in Section 7.1, the calculation is very brief, since it is direct and it does not need iterations or a thorough preliminary calculation. Indeed, in order to calculate the mechanical losses (21)–(22) we use the last between Eq. (3), Table 1 and Eq. (4). The powers flowing through the electric motors are then calculated by mean of Eqs. (26) and (27). Furthermore, the mathematical model used to analyze the two functional modes (shunt and compound) is the same. Indeed, only the value of the parameter $\tau_{\#o}$ has to be modified, because the mechanical losses and the real power flows, just like the ideal ones, depend only on the mechanical points.

9. Conclusions

An innovative approximate approach for the analysis of the mechanical losses of planetary transmissions, and specifically those employed in hybrid electric power-split CVTs, has been described. It can be used alone, or as a complement to the design and analysis methods published respectively in [16] and [48]. Thanks to its generality, it can be applied to any kind of PS-CVT, or to discrete planetary transmissions as well. Unlike the exact methods, it makes superfluous to segment the operating range in order to keep the model physically consistent. Moreover, for each target output speed and power, it permits calculating the speed and power of the three power units (i.e. of the i.c. engine and of the two electric machines) directly and by mean of general scheme-independent expressions.

Eventually, the proposed method has been applied to a real hybrid electric transmission. The errors in respect of the simulated transmission is negligible, especially considering the advantages of its easier and unified analytical implementation in respect of an exact method.

References

[1] AM. Kluger, D. Long, An Overview of Current Automatic, Manual and Continuously Variable Transmission Efficiencies and Their Projected Future Improvements, 1999 SAE Technical Paper 1999-01-1259, doi:10.4271/1999-01-1259.
[2] J.M. Miller, S.E. Schulz, B. Conlon, M. Duvall, M.D. Kankam, N. Nagel, Adjustable speed drives transportation industry needs part I: automotive, in: Veh. Technol. Conf. 2003, VTC 2003-Fall. 2003 IEEE 58th, 5, 2003, pp. 3220–3225.
[3] M. Pasquier, Continuously Variable Transmission Modifications and Control for a Diesel Hybrid Electric Powertrain, 2004 SAE Technical Paper 2004-08-23.
[4] G. Carbone, L. Mangialardi, G. Mantriota, A comparison of the performances of full and half toroidal traction drives, Mech. Mach. Theory 39 (2004) 921–942.
[5] M. Cammalleri, A new approach to the design of a speed-torque-controlled rubber V-belt variator, Proc. Inst. Mech. Eng. Part D 219 (2005) 1413–1427.

[6] M. Cammalleri, F. Sorge, Approximate closed-form solutions for the shift mechanics of rubber belt variators, Proceeding of ASME (IDETC 2009), August 30 - September 2, 2009, doi:10.1115/DETC2009-86638.
[7] N. Srivastava, I. Haque, A review on belt and chain continuously variable transmissions (CVT): Dynamics and control, Mech. Mach. Theory 44 (2009) 19–41.
[8] F. Sorge, M. Cammalleri, Helical shift mechanics of rubber V-Belt variators, J. Mech. Des. 133 (4) (2011), doi:10.1115/1.4003803.
[9] H. Naunheimer, B. Bertsche, J. Ryborz, W. Novak, Automotive Transmissions: Fundamentals, Selection, Design and Application, Springer-Verlag, Berlin, 2011.
[10] R. Fischer, F. Küçükay, G. Jürgens, R. Najork, B. Pollak, The Automotive Transmission Book, Springer International Publishing, Switzerland, 2015.
[11] A. Villeneuve, Dual Mode Electric Infinitely Variable Transmission, 2004 SAE Technical Paper 2004-40-0019.
[12] B. Conlon, Comparative analysis of single and combined hybrid electrically variable transmission operating modes, SAE World Congr. 2005 (2005).
[13] J.M. Miller, Hybrid electric vehicle propulsion system architectures of the e-CVT type, IEEE Trans. Power Electron. 21 (2006) 756–767.
[14] J.D. Wishart, Y. Zhou, Z. Dong, in: 19th Int. Conf. Des. Theory Methodol.; 1st Int. Conf. Micro- Nanosyst.; 9th Int. Conf. Adv. Veh. Tire Technol., 3, 2007, pp. 1091–1112.
[15] A. Sciarretta, L. Serrao, P.C. Dewangan, A control benchmark on the energy management of a plug-in hybrid electric vehicle, Control Eng. Pract 29 (2014) 287–298.
[16] M. Cammalleri, D. Rotella, Functional design of power-split CVTs: an uncoupled hierarchical optimized model, Mech. Mach. Theory 116 (2017) 294–309.
[17] E.I. Radzimovsky, A simplified approach for determining power losses and efficiencies of planetary gear drives, Mach. Des. (1956) 101–110.
[18] E.I. Radzimovsky, How to find efficiency, speed and power losses in planetary gear drives,, Mach. Des. (1959) 144–153.
[19] R.H. Macmillan, Power flow and loss in differential mechanisms, Proc. Inst. Mech. Eng. Part C J. Mech. Eng. Sci. 3 (1961) 37–41, doi:10.1243/JMES_JOUR_1961_003_007_02.
[20] J.W. Polder, A Universal Mathematical Model for Epicyclic Gear Trains, in: Gearing and transmissions: mechanisms conference and international symposium, 1972, San Francisco. - New York:, American Society of Mechanical Engineers (ASME), 1972, pp. 1–11.
[21] N. Beachley, D. Yu, Mechanical efficiency of differential gearing, Gear Technol. 48 (1986) 9–16 July/August 1986.
[22] E. Pennestrì, F. Freudenstein, The mechanical effieciency of epicyclic gear trains, J. Mech. Des. 115 (1993) 645–651.
[23] E. Pennestrì, L. Mariti, P.P. Valentini, V.H. Mucino, Efficiency evaluation of gearboxes for parallel hybrid vehicles: theory and applications, Mech. Mach. Theory. 49 (2012) 157–176, doi:10.1016/j.mechmachtheory.2011.10.012.
[24] R.H. Macmillan, P.B. Davies, Analytical study of systems for bifurcated power transmission, Proc. Inst. Mech. Eng. Part C J. Mech. Eng. Sci. 7 (1965) 40–47.
[25] A.K. Gupta, C.P. Ramanarayanan, Analysis of circulating power within hybrid electric vehicle transmissions, Mech. Mach. Theory. 64 (2013) 131–143, doi:10.1016/j.mechmachtheory.2013.01.011.
[26] G. White, Derivation of high efficiency two-stage epicyclic gears, Mech. Mach. Theory. 38 (2003) 149–159, doi:10.1016/S0094-114X(02)00093-9.
[27] A. Beccari, M. Cammalleri, Implicit regulation for automotive variators, Proc. Inst. Mech. Eng. Part D: J. Automob. Eng. 215 (2001) 697–708.
[28] M. Cammalleri, Efficiency of Split-Way CVT's. A simplified model, SAE Technical Papers 15 (2007), doi:10.4271/2007-24-0133.
[29] M.J. French, A Carnot theorem for split torque variable speed gears, Proc. Inst. Mech. Eng. Part C J. Mech. Eng. Sci. 10 (1968) 198–201.
[30] D.J. Sanger, The determination of power flow in multiple-path transmission systems, Mech. Mach. Theory. 7 (1972) 103–109, doi:10.1016/0094-114X(72)90020-1.
[31] F. Freudenstein, a.T. Yang, Kinematics and statics of a coupled epicyclic spur-gear train, Mech. Mach. Theory. 7 (1972) 263–275, doi:10.1016/0094-114X(72)90008-0.
[32] W. Wang, R. Song, M. Guo, S. Liu, Analysis on compound-split configuration of power-split hybrid electric vehicle, Mech. Mach. Theory. 78 (2014) 272–288, doi:10.1016/j.mechmachtheory.2014.03.019.
[33] E.L. Esmail, Efficiency evaluation of gearboxes for parallel hybrid vehicles: Theory and applications, Mech. Mach. Theory (2012) 157–176.
[34] A. AïtTaleb, A. Chaâba, M. Sallaou, Efficiency evaluation of continuously variable transmissions including a planetary gear train, Energy Power Eng. (2013) 153–160.
[35] L. Mangialardi, G. Mantriota, Power flows and efficiency in infinitely variable transmissions, Mech. Mach. Theory 34 (1999) 973–994, doi:10.1016/S0094-114X(98)00089-5.
[36] G. Mantriota, Performances of a series infinitely variable transmission with type I power flow, Mech. Mach. Theory. 37 (2002) 555–578, doi:10.1016/S0094-114X(02)00018-6.
[37] G. Mantriota, Performances of a parallel infinitely variable transmissions with a type II power flow, Mech. Mach. Theory. 37 (2002) 555–578, doi:10.1016/S0094-114X(02)00018-6.
[38] F. Bottiglione, Reversibility of power-split transmissions, J. Mech. Des. (2011).
[39] F. Bottiglione, S. De Pinto, G. Mantriota, Infinitely variable transmissions in neutral gear: torque ratio and power re-circulation, Mech. Mach. Theory. 74 (2014) 285–298, doi:10.1016/j.mechmachtheory.2013.12.017.
[40] C. Chen, J. Chen, Efficiency analysis of two degrees of freedom epicyclic gear transmission and experimental validation, Mech. Mach. Theory. 87 (2015) 115–130, doi:10.1016/j.mechmachtheory.2014.12.017.
[41] J.M. Del Castillo, The analytical expression of the efficiency of planetary gear trains, Mech. Mach. Theory 37 (2002) 197–214, doi:10.1016/S0094-114X(01)00077-5.
[42] D.R. Salgado, J.M. Del Castillo, Analysis of the transmission ratio and efficiency ranges of the four-, five-, and six-link planetary gear trains, Mech. Mach. Theory 73 (2014) 218–243, doi:10.1016/j.mechmachtheory.2013.11.001.
[43] P. Valentini, E. Pennestrì, A review of formulas for the mechanical efficiency analysis of two degrees-of-freedom epicyclic gear trains, J. Mech. Des. 125 (2003) 602–608, doi:10.1115/1.1587157.
[44] P.M.T. Marques, R.C. Martins, J.H.O. Seabra, Power loss and load distribution models including frictional effects for spur and helical gears, Mech. Mach. Theory. 96 (2016) 1–25, doi:10.1016/j.mechmachtheory.2015.09.005.
[45] G. Mantriota, Pennestrì, Theoretical and experimental efficiency analysis of multi degrees-of-freedom epicyclic gear trains, Multi- body Syst. Dyn 7 (2003) 389–406.
[46] L.P. Laus, H. Simas, D. Martins, Efficiency of gear trains determined using graph and screw theories, Mech. Mach. Theory 52 (2012) 296–325, doi:10.1016/j.mechmachtheory.2012.01.011.
[47] A. Kahraman, D.R. Hilty, A. Singh, An experimental investigation of spin power losses of a planetary gear set, Mech. Mach. Theory. 86 (2015) 48–61, doi:10.1016/j.mechmachtheory.2014.12.003.
[48] D. Rotella, M. Cammalleri, Direct analysis of power-split CVTs: a unified method, Mech. Mach. Theory 121 (2018) 116–127.
[49] A. Beccari, M. Cammalleri, F. Sorge, Experimental results for a two-mode split-way CVT, VDI Berichte 1709 (2002) 237–250.